

# Comparative study between PI, RST and sliding mode controllers of a DFIG supplied by an AC-AC converter for wind energy conversion system

\*Ahmed Bourouina, Abdelkader Chaker

Electrical Engineering Department ENP Oran, Algeria,  
Simulation, Commanded, Analysis and Maintenance  
Electrical Network.,

\*ahmed\_bourouina@yahoo.fr

\*\* Zinelaabidine Boudjema, Abdelkader Djahbar

Laboratoire Génie Electrique et Energies Renouvelables  
(LGEER), Electrical Engineering Department  
Hassiba Benbouali University, Chlef, Algeria.

\*\* Boudjema1983@yahoo.fr

**Abstract**—This paper deals with a variable speed device to produce electrical energy on a power network, based on a doubly-fed induction generator (DFIG) supplied by a direct matrix converter used in wind energy conversion systems. In the first place, we carried out briefly a study of modelling on the whole system. In order to control the power flowing between the stator of the DFIG and the power network, a control law is synthesized using three types of controllers: PI, RST and sliding mode controllers. Their respective performances are compared in terms of power reference tracking, response to sudden speed variations, sensitivity to perturbations and robustness against machine parameters variations.

**Keywords**—doubly fed induction motor (DFIM); power inverter; speed control; second order sliding mode.

## I. INTRODUCTION

Wind energy is the most promising renewable source of electrical power generation for the future. Many countries promote the wind power technology through various national programs and market incentives. Wind energy technology has evolved rapidly over the past three decades with increasing rotor diameters and the use of sophisticated power electronics to allow operation at variable speed [1].

Doubly fed induction generator (DFIG) is one of the most popular variable speed wind turbines in use nowadays. It is normally fed by a voltage source inverter. However, currently the three phase matrix converters have received considerable attention because they may become a good alternative to voltage-source inverter Pulse Width-Modulation (PWM) topology. This is because the matrix converter provides bi-directional power flow, nearly sinusoidal input/output waveforms, and a controllable input power factor. Furthermore, the matrix converter allows a compact design due to the lack of dc-link capacitors for energy storage. Consequently, in this work, a three-phase matrix converter is used to drive the DFIG.

In recent years, a lot of works have been presented with diverse control diagrams of DFIG. These control diagrams are usually based on vector control notion with conventional PI

controllers as proposed by Pena et al. in [2,3]. The similar conventional controllers are also used to realize control techniques of DFIG when grid faults appear like unbalanced voltages [4,5] and voltage dips [6]. It has also been shown in [7,8] that glimmer problems could be resolved with suitable control strategies. Many of these works prove that stator reactive power control can be an adapted solution to these diverse problems.

This paper discusses the control of electrical power exchanged between the stator of the DFIG and the power network by controlling independently the active and reactive powers. After modeling the whole system, active and reactive powers provided by the DFIG are controlled using three types of controllers: Integral-Proportional (PI), an RST controller based on pole placement theory and sliding mode. Their performances are compared in terms of reference tracking, sensitivity to perturbations and robustness against machine's parameters variations.

## II. SYSTEM MODELING

### A. Wind turbine model

For a horizontal axis wind turbine, the mechanical power captured from the wind is given by:

$$P_t = \frac{1}{2} C_p(\lambda, \beta) R^2 \rho v^3 \quad (1)$$

Where, R is the radius of the turbine (m),  $\rho$  is the air density (kg/m<sup>3</sup>), v is the wind speed (m/s), and  $C_p$  is the power coefficient which is a function of both tip speed ratio  $\lambda$ , and blade pitch angle  $\beta$  (deg). In this work, the  $C_p$  equation is approximated using a non-linear function according to [9].

$$C_p = (0.5 - 0.167)(\beta - 2) \sin \left[ \frac{\pi(\lambda + 0.1)}{18.5 - 0.3(\beta - 2)} \right] - 0.0018(\lambda - 3)(\beta - 2) \quad (2)$$

The tip speed ratio is given by:

$$\lambda = \frac{\Omega_t R}{v} \quad (3)$$

Where  $\Omega t$  is the angular velocity of Wind Turbine.

**B. The matrix converter model**

The matrix converter performs the power conversion directly from AC to AC without any intermediate dc link. It is very simple in structure and has powerful controllability. The converter consists of a matrix of bi-directional switches linking two independent three-phase systems. Each output line is linked to each input line via a bi-directional switch. Figure 1 shows the basic diagram of a matrix converter.

The switching function of a switch  $S_{mn}$  in figure 1 is given by :

$$S_{mn} = \begin{cases} 1 & S_{mn} \text{ closed} \\ 0 & S_{mn} \text{ open} \end{cases} \quad m \in \{A, B, C\}, n \in \{a, b, c\} \quad (4)$$

The mathematical expression that represents the operation of the matrix converter in figure 1 can be written as :

$$\begin{bmatrix} V_a \\ V_b \\ V_c \end{bmatrix} = \begin{bmatrix} S_{Aa} & S_{Ab} & S_{Ac} \\ S_{Ba} & S_{Bb} & S_{Bc} \\ S_{Ca} & S_{Cb} & S_{Cc} \end{bmatrix} \cdot \begin{bmatrix} V_A \\ V_B \\ V_C \end{bmatrix} \quad (5)$$

$$\begin{bmatrix} i_A \\ i_B \\ i_C \end{bmatrix} = \begin{bmatrix} S_{Aa} & S_{Ba} & S_{Ca} \\ S_{Ab} & S_{Bb} & S_{Cb} \\ S_{Ac} & S_{Bc} & S_{Cc} \end{bmatrix}^T \cdot \begin{bmatrix} i_a \\ i_b \\ i_c \end{bmatrix} \quad (6)$$

To determine the behavior of the matrix converter at output frequencies well below the switching frequency, a modulation duty cycle can be defined for each switch.

The input/output relationships of voltages and currents are related to the states of the nine switches and can be expressed as follows :

$$\begin{bmatrix} V_a \\ V_b \\ V_c \end{bmatrix} = \begin{bmatrix} k_{Aa} & k_{Ab} & k_{Ac} \\ k_{Ba} & k_{Bb} & k_{Bc} \\ k_{Ca} & k_{Cb} & k_{Cc} \end{bmatrix} \cdot \begin{bmatrix} V_A \\ V_B \\ V_C \end{bmatrix} \quad (7)$$

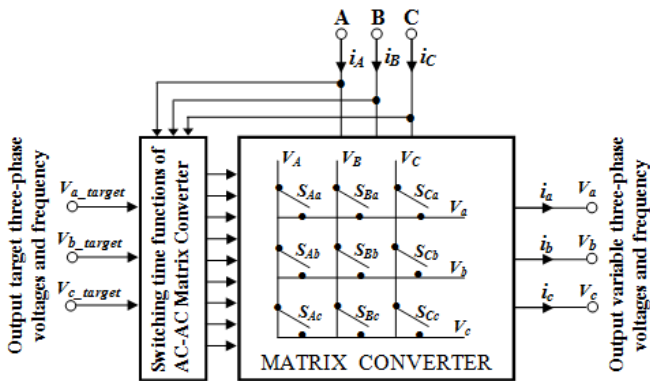


Fig. 1. Schematic representation of the matrix converter.

$$\begin{bmatrix} i_A \\ i_B \\ i_C \end{bmatrix} = \begin{bmatrix} k_{Aa} & k_{Ba} & k_{Ca} \\ k_{Ab} & k_{Bb} & k_{Cb} \\ k_{Ac} & k_{Bc} & k_{Cc} \end{bmatrix}^T \cdot \begin{bmatrix} i_a \\ i_b \\ i_c \end{bmatrix} \quad (8)$$

With :  $0 \leq k_{mn} \leq 1, \quad m = A, B, C, \quad n = a, b, c \quad (9)$

The variables  $k_{mn}$  are the duty cycles of the nine switches  $S_{mn}$  and can be represented by the duty-cycle matrix  $k$ . In order to prevent a short circuit on the input side and ensure uninterrupted load current flow, these duty cycles must satisfy the three following constraint conditions :

$$k_{Aa} + k_{Ab} + k_{Ac} = 1 \quad (10)$$

$$k_{Ba} + k_{Bb} + k_{Bc} = 1 \quad (11)$$

$$k_{Ca} + k_{Cb} + k_{Cc} = 1 \quad (12)$$

The high-frequency synthesis technique introduced by Venturini (1980) and Alesina and Venturini (1988), allows a control of the  $S_{mn}$  switches so that the low frequency parts of the synthesized output voltages ( $V_a, V_b$  and  $V_c$ ) and the input currents ( $i_a, i_b$  and  $i_c$ ) are purely sinusoidal with the prescribed values of the output frequency, the input frequency, the displacement factor and the input amplitude.

The output voltage is given by :

$$\begin{bmatrix} V_a \\ V_b \\ V_c \end{bmatrix} = \begin{bmatrix} 1+2\delta \cos \alpha & 1+2\delta \cos(\alpha - \frac{2\pi}{3}) & 1+2\delta \cos(\alpha - \frac{4\pi}{3}) \\ 1+2\delta \cos(\alpha - \frac{4\pi}{3}) & 1+2\delta \cos \alpha & 1+2\delta \cos(\alpha - \frac{2\pi}{3}) \\ 1+2\delta \cos(\alpha - \frac{2\pi}{3}) & 1+2\delta \cos(\alpha - \frac{4\pi}{3}) & 1+2\delta \cos \alpha \end{bmatrix} \cdot \begin{bmatrix} V_A \\ V_B \\ V_C \end{bmatrix} \quad (13)$$

Where :  $\begin{cases} \alpha = \omega_m + \theta \\ \omega_m = \omega_{output} - \omega_{input} \end{cases}$

The running matrix converter with Venturini algorithm generates at the output a three-phases sinusoidal voltages system having in that order pulsation  $\omega_m$ , a phase angle  $\theta$  and amplitude  $\delta \cdot V_s$  ( $0 < \delta < 0.866$  with modulation of the neural) [10].

**C. The DFIG model**

The application of Concordia and Park's transformation to the three-phase model of the DFIG permits to write the dynamic voltages and fluxes equations in an arbitrary  $d-q$  reference frame:

$$\begin{cases} V_{ds} = R_s I_{ds} + \frac{d}{dt} \psi_{ds} - \omega_s \psi_{qs} \\ V_{qs} = R_s I_{qs} + \frac{d}{dt} \psi_{qs} + \omega_s \psi_{ds} \\ V_{dr} = R_r I_{dr} + \frac{d}{dt} \psi_{dr} - \omega_r \psi_{qr} \\ V_{qr} = R_r I_{qr} + \frac{d}{dt} \psi_{qr} + \omega_r \psi_{dr} \end{cases} \quad \begin{cases} \psi_{ds} = L_s I_{ds} + M I_{dr} \\ \psi_{qs} = L_s I_{qs} + M I_{qr} \\ \psi_{dr} = L_r I_{dr} + M I_{ds} \\ \psi_{qr} = L_r I_{qr} + M I_{qs} \end{cases} \quad (14)$$

The stator and rotor angular velocities are linked by the following relation :  $\omega_s = \omega + \omega_r$ .

This electrical model is completed by the mechanical equation:

$$C_{em} = C_r + J \frac{d\Omega}{dt} + f\Omega \quad (15)$$

Where the electromagnetic torque  $C_{em}$  can be written as a function of stator fluxes and rotor currents :

$$C_{em} = p \frac{M}{L_s} (\psi_{qs} I_{dr} - \psi_{ds} I_{qr}) \quad (16)$$

### III. CONTROL STRATEGY OF THE DFIG

In order to easily control the production of electricity by the wind turbine, we will carry out an independent control of active and reactive powers by orientation of the stator flux. This orientation will be made in this work with a real model of the DFIG, i.e. without negligence of the stator resistance [11,12].

By choosing a reference frame linked to the stator flux, rotor currents will be related directly to the stator active and reactive power. An adapted control of these currents will thus permit to control the power exchanged between the stator and the grid. If the stator flux is linked to the d-axis of the frame we have:

$$\psi_{ds} = \psi_s \quad \text{and} \quad \psi_{qs} = 0 \quad (17)$$

And the electromagnetic torque can then be expressed as :

$$C_{em} = -p \frac{M}{L_s} I_{qr} \psi_{ds} \quad (18)$$

By substituting Eq.17 in Eq.14, the following rotor flux equations are obtained :

$$\begin{cases} \psi_s = L_s I_{ds} + M I_{dr} \\ 0 = L_s I_{qs} + M I_{qr} \end{cases} \quad (19)$$

In addition, the stator voltage equations are reduced to:

$$\begin{cases} V_{ds} = R_s I_{ds} + \frac{d}{dt} \psi_s \\ V_{qs} = R_s I_{qs} + \omega_s \psi_s \end{cases} \quad (20)$$

By supposing that the electrical supply network is stable, having for simple voltage  $V_s$ , which led to a stator flux  $\psi_s$  constant. This consideration associated with Eq.18 shows that the electromagnetic torque only depends on the  $q$ -axis rotor current component. With these assumptions, the new stator voltage expressions can be written as follows:

$$\begin{cases} V_{ds} = R_s I_{ds} \\ V_{qs} = R_s I_{qs} + \omega_s \psi_s \end{cases} \quad (21)$$

Using Eq.19, a relation between the stator and rotor currents can be established :

$$\begin{cases} I_{ds} = -\frac{M}{L_s} I_{dr} + \frac{\psi_s}{L_s} \\ I_{qs} = -\frac{M}{L_s} I_{qr} \end{cases} \quad (22)$$

The stator active and reactive powers are written:

$$\begin{cases} P_s = V_{ds} I_{ds} + V_{qs} I_{qs} \\ Q_s = V_{qs} I_{ds} - V_{ds} I_{qs} \end{cases} \quad (23)$$

By using Eqs.14, 17, 22 and 23, the statoric active and reactive power, the rotoric fluxes and voltages can be written versus rotoric currents as:

$$\begin{cases} P_s = \frac{\omega_s \psi_s M}{L_s} I_{qr} - \frac{V_s^2}{R_s} + \frac{\omega_s^2 \psi_s^2}{R_s} \\ Q_s = -\frac{\omega_s \psi_s M}{L_s} I_{dr} + \frac{\omega_s \psi_s^2}{L_s} \end{cases} \quad (24)$$

$$\begin{cases} \psi_{dr} = (L_r - \frac{M^2}{L_s}) I_{dr} + \frac{M \psi_s}{L_s} \\ \psi_{qr} = (L_r - \frac{M^2}{L_s}) I_{qr} \end{cases} \quad (25)$$

$$\begin{cases} V_{dr} = R_r I_{dr} + (L_r - \frac{M^2}{L_s}) \frac{dI_{dr}}{dt} - g\omega_s (L_r - \frac{M^2}{L_s}) I_{qr} \\ V_{qr} = R_r I_{qr} + (L_r - \frac{M^2}{L_s}) \frac{dI_{qr}}{dt} + g\omega_s (L_r - \frac{M^2}{L_s}) I_{dr} + g\omega_s \frac{M \psi_s}{L_s} \end{cases} \quad (26)$$

In steady state, the second derivative terms of the two equations in 27 are equal to zero. We can thus write:

$$\begin{cases} V_{dr} = R_r I_{dr} - g\omega_s (L_r - \frac{M^2}{L_s}) I_{qr} \\ V_{qr} = R_r I_{qr} + g\omega_s (L_r - \frac{M^2}{L_s}) I_{dr} + g\omega_s \frac{M \psi_s}{L_s} \end{cases} \quad (28)$$

The third term, which constitutes cross-coupling terms, can be neglected because of their small influence. These terms can be compensated by an adequate synthesis of the regulators in the control loops.

### IV. CONTROLLERS SYNTHESIS

In this section, we have chosen to compare the performances of the DFIG with three different controllers: *PI*, *RST* and sliding mode

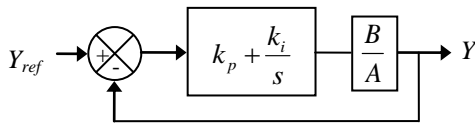


Fig. 2. System with PI controller.

Based on relations (22), (24) and (27), the control system can be designed as shown in figure 1. The blocks  $R_1$ ,  $R_2$ ,  $R_3$  and  $R_4$  represent respectively the stator powers and the rotor currents regulators.

A. PI regulator synthesis

This controller is simple to elaborate. Figure 2 shows the block diagram of the system implemented with this controller. The terms  $k_p$  and  $k_i$  represent respectively the proportional and integral gains. The quotient  $B/A$  represents the transfer function to be controlled, where  $A$  and  $B$  are presently defined as follows:

$$A = L_s R_r + s \cdot L_s \left( L_r - \frac{M^2}{L_s} \right) \text{ and } B = \omega_s \psi_s M \tag{28}$$

The regulator terms are calculated with a pole-compensation method. The time response of the controlled system will be fixed at 10 ms. This value is sufficient for our application and a lower value might involve transients with important overshoots. The calculated terms are:

$$k_i = \frac{1}{1 \times 10^{-3}} \frac{L_s R_r}{M \omega_s \psi_s}, \quad k_p = \frac{1}{1 \times 10^{-3}} \frac{L_s \left( L_r - \frac{M^2}{L_s} \right)}{M \omega_s \psi_s} \tag{29}$$

It is important to specify that the pole-compensation is not the only method to calculate a PI regulator but it is simple to elaborate with a first-order transfer-function and it is sufficient in our case to compare with other regulators.

B. RST controller synthesis

The block-diagram of a system with its RST controller is presented on figure 3 [13].

The system with the transfer-function  $B/A$  has  $Y_{ref}$  as reference and is disturbed by the variable  $\gamma$ .  $R$ ,  $S$  and  $T$  are polynomials which constitutes the controller. In our case, we have:

$$A = L_s R_r + s \cdot L_s \left( L_r - M^2/L_s \right) \text{ and } B = M V_s \tag{30}$$

Where  $s$  is the Laplace operator.

The transfer-function of the regulated system is :

$$Y = \frac{BT}{AS + BR} Y_{ref} + \frac{BS}{AS + BR} \gamma \tag{31}$$

By applying the Besout equation, we put :

$$D = AS + BR = CF \tag{32}$$

Where  $C$  is the command polynomial and  $F$  is the filtering polynomial. In order to have a good adjustment accuracy, we choose a strictly proper regulator. So if  $A$  is a polynomial of  $n$  degree ( $\deg(A)=n$ ) we must have :

$$\deg(D)=2n+1, \quad \deg(S)=\deg(A)+1, \quad \deg(R)=\deg(A)$$

In our case :

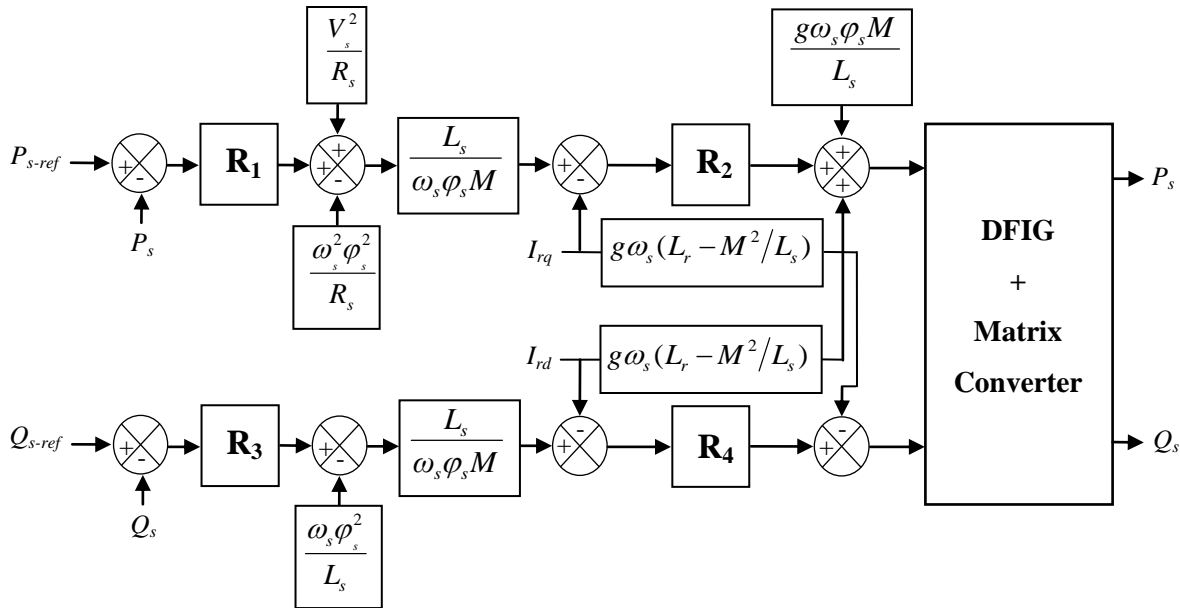


Fig. 3. Power control of the DFIG.

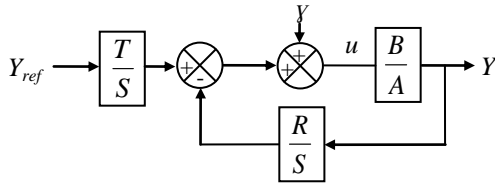


Fig. 4. Block diagram of the RST controller.

$$\begin{cases} A = a_1s + a_0 & ; R = r_1s + r_0 \\ B = b_0 & ; S = s_2s^2 + s_1s + s_0 \\ D = d_3s^3 + d_2s^2 + d_1s + a_0 \end{cases} \quad (33)$$

To find the coefficients of polynomials  $R$  and  $S$ , the robust pole placement method is adopted with  $T_c$  as control horizon and  $T_f$  as filtering horizon [9]. We have:

$$p_c = -\frac{1}{T_c} \text{ and } p_f = -\frac{1}{T_f} \quad (34)$$

Where  $p_c$  is the pole of  $C$  and  $p_f$  the double pole of  $F$ . The pole  $p_c$  must accelerate the system and is generally chosen three to five times greater than the pole of  $A$   $p_a$ .  $p_f$  is generally chosen three times smaller than  $p_c$ . In our case:

$$T_c = \frac{1}{3}T_f = -\frac{1}{3p_a} = \frac{L_s(L_r - M^2/L_s)}{5L_sR_r} \quad (35)$$

Perturbations are generally considered as piecewise constant.  $y$  can then be modelled by a step input. To obtain good disturbance rejections, the final value theorem indicate that the term  $BS/(AS + BR)$  must tend towards zero:

$$\lim_{s \rightarrow 0} \frac{S}{D} \gamma = 0 \quad (36)$$

To obtain a good stability in steady-state, we must have  $D(0) \neq 0$  and respect relation (36). The Bezout equation leads to four equations with four unknown terms where the coefficients of  $D$  are related to the coefficients of polynomials  $R$  and  $S$  by the Sylvester Matrix :

$$\begin{pmatrix} d_3 \\ d_2 \\ d_1 \\ d_0 \end{pmatrix} = \begin{pmatrix} a_1 & 0 & 0 & 0 \\ 0 & a_1 & 0 & 0 \\ 0 & 0 & b_0 & 0 \\ 0 & 0 & 0 & b_0 \end{pmatrix} \begin{pmatrix} s_2 \\ s_1 \\ r_1 \\ r_0 \end{pmatrix} \quad (37)$$

In order to determine the coefficients of  $T$ , we consider that in steady state  $Y$  must be equal to  $Y_{ref}$  so:

$$\lim_{s \rightarrow 0} \frac{BT}{AS + BR} = 1 \quad (38)$$

As we know that  $S(0)=0$ , we conclude that  $T=R(0)$ . In order to separate regulation and reference tracking, we try to

make the term  $BT/(AS + BR)$  only dependent on  $C$ . We then consider  $T=hF$  (where  $h$  is real) and we can write:

$$\frac{BT}{AS + BR} = \frac{BT}{D} = \frac{BhF}{CF} = \frac{Bh}{D} \quad (39)$$

As  $T=R(0)$ , we conclude that  $h = R(0)/F(0)$ .

### C. Sliding mode controller synthesis

The sliding mode is a technique to adjust feedback by previously defining a surface. The system which is controlled will be forced to that surface, then the behaviour of the system slides to the desired equilibrium point [14]. The main feature of this control is that we only need to drive the error to a “switching surface”. When the system is in “sliding mode”, the system behaviour is not affected by any modelling uncertainties and/or disturbances. The design of the control system will be demonstrated for a nonlinear system presented in the canonical form [15,16]:

$$\dot{x} = f(x,t) + B(x,t)V(x,t), x \in R^n, V \in R^m, \text{ran}(B(x,t)) = m \quad (40)$$

With control in the sliding mode, the goal is to keep the system motion on the manifold  $S$ , which is defined as:

$$S = \{x : e(x, t) = 0\} \quad (41)$$

$$e = x^d - x \quad (42)$$

Here  $e$  is the tracking error vector,  $x^d$  is the desired state,  $x$  is the state vector. The control input  $u$  has to guarantee that the motion of the system described in (40) is restricted to belong to the manifold  $S$  in the state space. The sliding mode control should be chosen such that the candidate Lyapunov function satisfies the Lyapunov stability criteria :

$$\mathcal{G} = \frac{1}{2}S(x)^2, \quad \dot{\mathcal{G}} = S(x)\dot{S}(x). \quad (43)$$

This can be assured for:

$$\dot{\mathcal{G}} = -\eta|S(x)| \quad (44)$$

Here  $\eta$  is strictly positive. Essentially, equation (43) states that the squared “distance” to the surface, measured by  $e(x)^2$ , decreases along all system trajectories. Therefore (44) satisfy the Lyapunov condition. With selected Lyapunov function the stability of the whole control system is guaranteed. The control function will satisfy reaching conditions in the following form:

$$V^{com} = V^{eq} + V^n \quad (45)$$

Here  $V^{com}$  is the control vector,  $V^{eq}$  is the equivalent control vector,  $V^n$  is the correction factor and must be calculated so that the stability conditions for the selected control are satisfied.

$$V^n = K \text{sat}((S(x)/\delta)) \quad (46)$$

Sat  $((S(x)/\delta))$  is the proposed saturation function,  $\delta$  is the boundary layer thickness. In this paper we propose the Slotine method [17]:

$$S(X) = \left( \frac{d}{dt} + \lambda \right)^{n-1} e \quad (47)$$

Here,  $e$  is the tracking error vector,  $\lambda$  is a positive coefficient and  $n$  is the relative degree.

In our study, we choose the error between the measured and references stator powers as sliding mode surfaces, so we can write the following expression:

$$\begin{cases} S_d = P_{S-ref} - P_s \\ S_q = Q_{S-ref} - Q_s \end{cases} \quad (48)$$

The first order derivate of (48), gives :

$$\begin{cases} \dot{S}_d = \dot{P}_{S-ref} - \dot{P}_s \\ \dot{S}_q = \dot{Q}_{S-ref} - \dot{Q}_s \end{cases} \quad (49)$$

Replacing the powers in (49) by their expressions given in (24), one obtains [18]:

$$\begin{cases} \dot{S}_1 = \dot{P}_{S-ref} - \frac{\omega_s \psi_s M}{L_s} \dot{I}_{qr} \\ \dot{S}_2 = \dot{Q}_{S-ref} + \frac{\omega_s \psi_s M}{L_s} \dot{I}_{dr} - \frac{\omega_s \psi_s^2}{L_s} \end{cases} \quad (50)$$

$V_{dr}$  and  $V_{qr}$  will be the two components of the control vector used to constraint the system to converge to  $S_{dq}=0$ . The control vector  $V_{dqeq}$  is obtained by imposing  $\dot{S}_{dq}=0$  so the equivalent control components are given by the following relation :

$$V_{dqeq} = \begin{bmatrix} -\frac{L_s \left( L_r - \frac{M^2}{L_s} \right)}{\omega_s \psi_s M} \dot{Q}_s^* + R_r I_{dr} - \left( L_r - \frac{M^2}{L_s} \right) g \omega_s I_{qr} + \frac{\left( L_r - \frac{M^2}{L_s} \right) \psi_s}{M} \\ \frac{L_s}{\omega_s \psi_s M} \dot{P}_s^* + R_r I_{qr} - \left( L_r - \frac{M^2}{L_s} \right) g \omega_s I_{dr} + \frac{g \omega_s \psi_s M}{L_s} \end{bmatrix} \quad (51)$$

To obtain good performances, dynamic and commutations around the surfaces, the control vector is imposed as follows :

$$V_{dq} = V_{dqeq} + K \cdot \text{sat}(S_{dq}) \quad (52)$$

The sliding mode will exist only if the following condition is met :

$$S \cdot \dot{S} < 0 \quad (53)$$

## V. SIMULATION RESULTS AND DISCUSSIONS

In this section, simulations are realized with a 5 KW generator coupled to a 380V/50Hz grid. Parameters of the machine are given in table 1. In the aim to evaluate the performances of the three controllers, three categories of tests have been realized: pursuit test, sensitivity to the speed variation and robustness against machine parameter variations

### A. Pursuit test

This test has for goal the study of the three controller's behaviors in reference tracking, while the machine's speed is considered constant at its nominal value. The simulation results are presented in figure 4. As it's shown by this figure, for the three controllers, the active and reactive generated powers track their references. In addition and contrary to the PI controller where the coupling effect between the two axes is very clear, we can notice that the RST and SMC controllers ensures a perfect decoupling between them. Therefore we can consider that these controllers have a good performance for this test.

### B. Sensitivity to the speed variation

The aim of this test is to analyze the influence of a speed variation of the DFIG on active and reactive powers for the three controllers. For this objective and at time  $t = 3s$ , the speed was varied from 150 rad/s to 170 rad/s (Figure 6). The simulation results are shown in figure 7. This figure express that the speed variation produced a slight effect on the powers curves of the three controllers. This result is attractive for wind energy applications to ensure stability and quality of the generated power when the speed is varying.

TABLE I. MACHINE PARAMETERS.

Parameters	Value	IS-Unit
Nominal power	5	KW
Stator voltage	380	V
Stator frequency	50	Hz
Number of pairs poles	3	
Nominal speed	150	rad/s
Stator resistance	0.95	$\Omega$
Rotor resistance	1.8	$\Omega$
Stator inductance	0.094	H
Rotor inductance	0.088	H
Mutual inductance	0.082	H

### C. Robustness

In order to test the robustness of the used controllers, the stator and the rotor resistances  $R_s$  and  $R_r$  are doubled and the values of inductances  $L_s$ ,  $L_r$  and  $M$  are divided by 2. The machine is running at its nominal speed. The results presented in figure 8 show that parameters variations of the DFIG increase slightly the time-response of the RST controller. On the other hand this results show that parameter variations of the DFIG presents a clear effect on the powers curves (their errors curves) and that the effect appears more significant for PI and RST controllers than that with SMC one. Thus it can be concluded that this last is the most robust among the proposed controllers studied in this work.

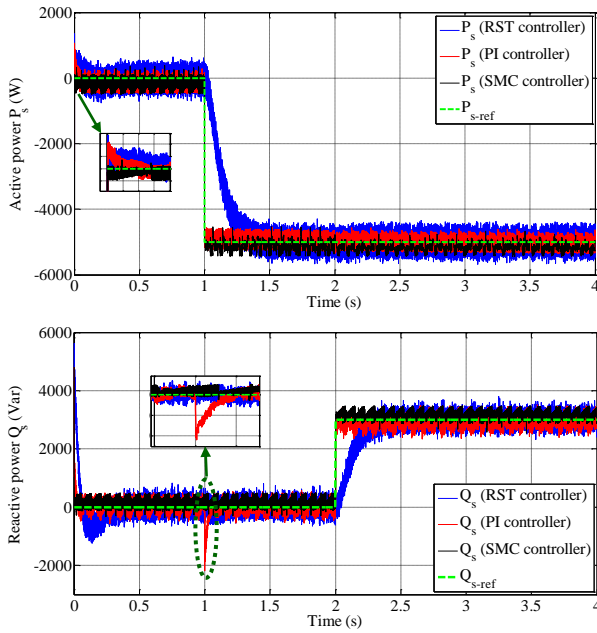


Fig. 5. Reference tracking.

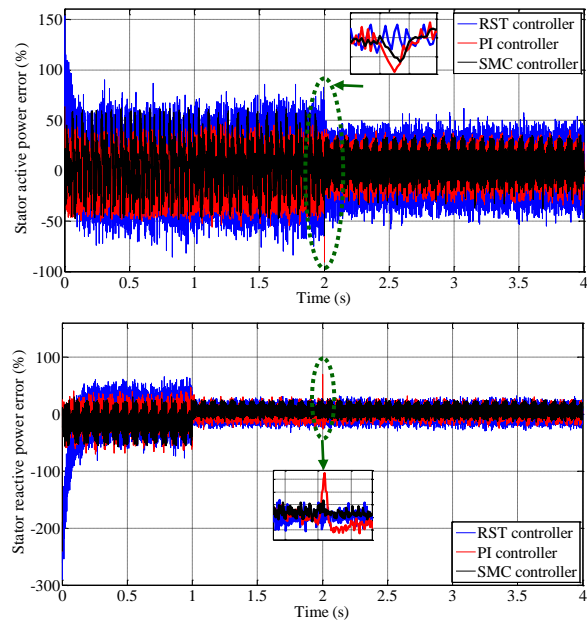


Fig. 8. Sensitivity to the DFIG's parameters variation on the DFIG control.

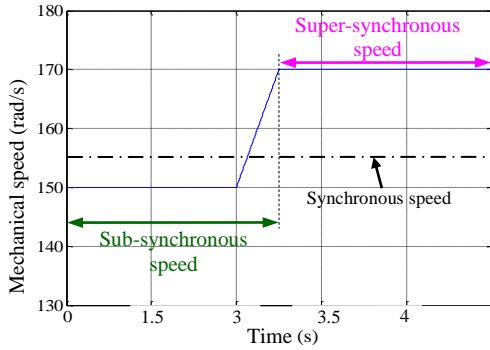


Fig. 6. Mechanical speed profile.

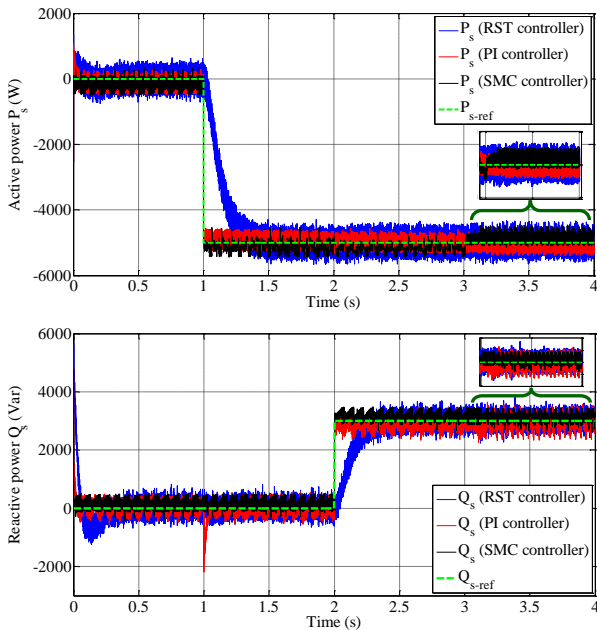


Fig. 7. Sensitivity to the speed variation.

VI. CONCLUSION

The modeling, the control and the simulation of an electrical power electromechanical conversion system based on the doubly fed induction generator (DFIG) connected directly to the grid by the stator and fed by a direct matrix converter on the rotor side has been presented in this study. Our objective was the implementation of a robust decoupled control system of active and reactive powers generated by the stator side of the DFIG, in order to ensure of the high performance and a better execution of the DFIG, and to make the system insensible with the external disturbances and the parametric variations. In the first step, we started with a study of modeling on the doubly fed induction generator.

In the first step, we started with a study of modeling on the matrix converter controlled by the Venturini modulation technique. In second step, we adopted a vector control strategy in order to control the stator active and reactive powers exchanged between the DFIG and the grid. Contrary to the previous work carried out on the DFIG where the researchers always neglect the stator resistance to facilitate its control, in our work this resistance was not neglected in order to return the system studied near to reality. In third step, three different controllers are synthesized and compared. In term of power reference tracking with the DFIG in ideal conditions (no parameters variations and no disturbances), the SMC and RST controllers ensure a perfect decoupling between the two axes comparatively to the PI one where the coupling effect between them is very clear.

When the machine's speed is modified (which represents a perturbation for the system), the impact on the active and reactive powers values is almost negligible for the three controllers. A robustness test has also been investigated where the machine parameters have been modified. These changes induce some disturbances on the powers responses but with an

effect almost doubled with the PI and RST controllers than on that with SMC one.

Basing on all these results it can be concluded that robust control method as SMC can be a very attractive solution for devices using DFIG such as wind energy conversion systems.

#### REFERENCES

- [1] O. Anaya-Lara, N. Jenkins, J. Ekanayake, P. Cartwright, M. Hughes, "Wind energy generation," In: Wiley, 2009.
- [2] R. Pena, J. C. Clare, G. M. Asher, "A doubly fed induction generator using back to back converters supplying an isolated load from a variable speed wind turbine," In: IEE Proceeding on Electrical Power Applications 143, pp. 380-387, September 5, 1996.
- [3] F. Wu, X. P.Zhang , P. Ju, and M. J. H.Sterling, " Decentralized Nonlinear Control of Wind Turbine With Doubly Fed Induction Generator,"In: IEEE TRANS ON POWER SYSTEMS, VOL. 23, NO. 2, pp. 613-621, MAY 2008.
- [4] M. A.Poller, " Doubly-fed induction machine models for stability assessment of wind farms," In: Power Tech Conference Proceedings, 2003, IEEE, Bologna, vol. 3, 23–26, June 2003.
- [5] T. Brekken and N. Mohan, "A novel doubly-fed induction wind generator control scheme for reactive power control and torque pulsation compensation under unbalanced grid voltage conditions,"In: IEEE 34<sup>th</sup> Annual Power Electronics Specialist Conference, 2003, PESC'03, Vol. 2, pp. 760-764, 15-19 June 2003.
- [6] T. Brekken and N. Mohan, "Control of a doubly fed induction wind generator under unbalanced grid voltage conditions," In: IEEE Transaction on Energy Conversion, 22 March, 2007 129–135.
- [7] J. Lopez, P. Sanchis, X. Roboam and L. Marroyo, "Dynamic behavior of the doubly fed induction generator during three-phase voltage dips," In: IEEE Transaction on Energy Conversion, pp. 709-717, 22 (September (3)) 2007.
- [8] T. Sun, Z. Chen and F. Blaabjerg, "Flicker study on variable speed wind turbines with doubly fed induction generators," In: IEEE Transactions on Energy Conversion, pp. 896–905, 20 (December (4)) 2005.
- [9] E.S. Abdin, W. Xu, "Control design and Dynamic Performance Analysis of a Wind Turbine Induction Generator Unit," IEEE Trans. On Energy conversion, vol.15, No1, March 2000.
- [10] M. Venturini "A new sine wave in sine wave out conversion technique which eliminates reactive elements," In: Proc Powercon 7, San Diego, CA, pp E3-1, E3-15, 27-24 March 1980.
- [11] Z. Boudjema, A. Meroufel and A.Amari, "Robust Control of a Doubly Fed Induction Generator (DFIG) Fedby a Direct AC-AC Converter," Przegład Elektrotechniczny, R. 88 NR 12a/2012, 213-221.
- [12] Xu.Hailiang, Hu. Jiabing and He.Yikang , "Operation of Wind-Turbine-Driven DFIG Systems Under Distorted Grid Voltage Conditions Analysis and Experimental Validations,"In: IEEE TRANSACTIONS ON POWER ELECTRONICS, VOL. 27, NO. pp. 2354-2366. 5, MAY 2012.
- [13] F. Poitier, T. Bouaouiche and M. Machoum, " Advanced control of a doubly-fed induction generator for wind energy conversion," Electric Power Systems Research 79 (2009) 1085–1096.
- [14] R. J. Wai and J. M. Chang, "Implementation of robust wavelet-neural-network sliding-mode control for induction servo motor drive," In: IEEE Trans. On Industrial Electronics, Vol. 50, No. 6, pp. 1317-1334, December 2003.
- [15] Z. Yan, C. Jin, V. I. Utkin, " Sensorless Sliding-Mode Control of Induction Motors,"In: IEEE Trans. Ind. electronic. 47 No. pp.1286-1297, 6 (December 2000), 1286–1297.
- [16] T. Sun, Z. Chen and F. Blaabjerg, "Flicker study on variable speed wind turbines with doubly fed induction generators," In: IEEE Transactions on Energy Conversion, pp. 896–905, 20 (December (4)) 2005.
- [17] J. J. E. Slotine and W. Li, "Applied Nonlinear Control," Englewood Cliffs, NJ: Prentice–Hall, 1991.
- [18] Z. Boudjema, A. Meroufel and Y. Djerriri, "Nonlinear control of a doubly fed induction generator for wind energy conversion," In: Carpathian Journal of Electronic and Computer Engineering, Vol. 6, No.1,2013.